Model selection during sample-standard-bracketing using reversible jump Markov Chain Monte Carlo

Journal:	*Journal of Analytical Atomic Spectrometry*
Manuscript ID:	JA-ART-03-2015-000102.R1
Article Type:	Paper
Date Submitted by the Author:	07-Aug-2015

Complete List of Authors:	Fox, Matthew; UC Berkeley, Earth and Planetary Science Ickert, Ryan; Berkeley Geochronology Center,

Model selection during sample-standard-bracketing using reversible jump Markov Chain Monte Carlo

Matthew Fox and Ryan B Ickert

Berkeley Geochronology Center and University of California, Berkeley

Corresponding Author: Matthew Fox (matthew.fox@berkeley.edu)

Abstract

For instrument calibration where interpolation between reference materials is required, there exists a need for a generally applicable technique to determine: 1) The value of the calibration (e.g., the mass bias at an arbitrary time); 2) The uncertainty of this value; and, 3) The degree to which the uncertainties in the reference material analyses account for their scatter about the calibration. Here, we show that an implementation of the reversible-jump Markov Chain Monte Carlo (rj-MCMC) technique can provide all three values for a reasonable range of complexity. Using this algorithm we treat a drifting calibration value as a function of time by a series of straight line segments. The benefit of the rj-MCMC technique is that the number of straight line segments does not need to be specified *a priori*, but is a parameter that is estimated. This technique is also able to simultaneously determine the presence and magnitude of overdispersion (the amount of scatter in the data not accounted for by estimated uncertainties) even in the presence of complex, non-linear drift. The result of this data treatment is a probability distribution in calibration-time space that, despite having an origin in line segments, smoothly follows the data and therefore yields the calibration value and its uncertainty. We validate this technique using synthetic data from prescribed distributions, and demonstrate its utility and flexibility by applying it to data collected by multi-collector inductively coupled plasma mass spectrometry that display complex non-linear drift.

Introduction

When making measurements of relative isotopic or elemental abundances by mass spectrometry there is usually a difference between the relative ion beam intensities - a directly measured quantity - and the quantity of interest, the relative abundances of the isotopes in the sample. In the absence of spectral interferences, this effect is most generally referred to as mass discrimination[1] or when specifically referring to isotopes of the same element, it is often called mass bias or mass fractionation. Correction for this effect is commonly made by measuring reference materials (RMs) interspersed with measurements of samples during an analytical session, a technique commonly referred to as sample-standard bracketing (SSB). This is a widely employed technique for the calibration of mass bias and relative sensitivity factors for mass spectrometers, particularly secondary ion mass spectrometry (SIMS[2,3]) and multi-collector inductively coupled plasma mass spectrometry (MC-ICPMS[4,5]).

In many cases, the calibration of mass discrimination in mass spectrometers drifts with time, making it necessary to make multiple calibration measurements during an analytical session to allow accurate interpolation between RM measurements. The way that time-dependent SSB data are treated is often related to the technique that is employed. For example, mass discrimination in ICPMS instruments may have significant fluctuations at timescales of minutes to hours[6], and therefore to achieve the highest accuracy, each sample must be bracketed by measurements of RMs in order to capture high-frequency variability. Alternatively, SIMS instruments tend to be very stable over several hours, and often the calibration may be indistinguishable from a single value for the duration of an analytical session[3]. In the latter case, accurate analyses can be achieved with lower frequency sampling of the mass discrimination.

Although the statistical tools currently in use by the mass spectrometry community are sufficient to produce good quality data, it is clear that improvements can be made. For example, in some SIMS and MC-ICPMS measurements, it is common practice to use only two bracketing analyses of RM to calibrate a single sample analysis by using a linear model interpolated between this pair of measurements. This approach assumes that the mean of the RM measurement is the true mean composition of the RM and that differences between RM are due only to instrument drift. Therefore, any error associated with the measurement of the RM directly leads to error in the data. In practice, other (non-bracketing) analyses of RM during the same analytical session will have a conditional relationship with the pair of bracketing RM, and could therefore enable the level of noise, or overdispersion, in the RM measurements to be assessed.

To the best of our knowledge, there is no technique available in the literature that is able to provide a straightforward method of model selection and overdispersion calculation for drifting calibration data. Paton et al.[7] describe a technique to determine overdispersion on drifting data using jackknife cross-validation technique, but their data were corrected using a spline fit. Compston and Clement[8] utilized a locally weighted least squares technique and a bootstrap to account for drifting data and it's uncertainty, but make no provision for overdisperson. Here, we provide an approach to infer the probability distribution of calibration drift through time along with an estimate of the overdispersion of the measured RM (the degree to which the uncertainties account for scatter in the data). In order to quantify this probability and simultaneously determine the complexity of the model, we use a reversible jump Markov chain Monte Carlo algorithm, a flexible numerical technique (e.g., Sambridge et al. [9]).

Interpolation using bracketing procedures

Figure 1 provides an illustration of ambiguity associated with model selection when interpolation between RM analyses is required for instrument calibration. We show twenty-seven measurements of the apparent $^{208}Pb/^{206}Pb$ of the reference material NIST SRM-612 glass by laser-ablation MC-ICPMS taken over the course of a ~7 hour analytical session (Figure 1a). These analyses are used to calibrate the instrument for the sample analyses that take place between sets of RM measurements. The total range of Pb isotopic compositions is about 0.1%, an order of magnitude larger than the uncertainties on individual analyses. The scatter in excess of the analytical uncertainties is not random: from inspection of Fig. 1a, it is clear that the Pb compositions rise for about the first ⅓ of the session, appear to either peak or are constant in the middle of the session, and then drop for the last half of the session. These smooth variations in mass discrimination are common on ICPMS instruments[6], where they probably reflect small changes in analytical conditions (expansion and contraction of components due to temperature changes, change in gas flow etc.). Unfortunately, there is no theory that predicts the form of the mass discrimination variation, nor is the drift reproducible from session to session in such a way that it can be predicted empirically.

We illustrate two commonly used methods to calculate mass bias corrections from these RM analyses.

The first method is by linear interpolation between each set of bracketing RMs and is illustrated in Fig. 1b. The advantage of this technique is that it is flexible and can account for nearly any form of drift because it only utilizes adjacent pairs of analyses, provided that there is no variation in the mass bias at a higher frequency than the RMs are measured. The main disadvantage is that it is an inefficient use of available data - by ignoring all but two analyses, the calibration is very sensitive to noise in the RM measurements and does not take into account the information provided by preceding and anteceding measurements. Furthermore, this method makes it difficult to determine the degree to which the estimated RM uncertainties account for scatter in the mass bias calibration, because each bracket is a line fit to two points, which by definition fit the data perfectly. This problem is ameliorated in analyses in which there is a large quantity of homogeneous sample available such that the measurement can be reproduced multiple times. However, for analyses that cannot be repeated - microbeam measurements where small-length-scale heterogeneities are of interest, for example - estimating overdispersion of RMs is a crucial element of estimating the correct uncertainty of samples.

A second method is to break the analytical session into segments that may be defined by arbitrary functions defined by the analyst, shown in Fig. 1c. For example, this analytical session could be broken into three different functions: 1) linear increase in the Pb isotopic composition through time; 2) constant through time; and 3) linear decrease in the Pb isotopic composition through time. These are illustrated in Figure 1. Unfortunately, the segmentation is arbitrary and cumbersome, induces sharp changes in the modelled mass discrimination, and can be challenging for more strongly non-linear drift.

Methods

Here we present a method to infer the calibration and its uncertainty as a function of time during an analytical session. We also use this method to simultaneously determine the overdispersion of the data. In order to describe calibration drift through time we treat the calibration as a series of straight-line segments that change slope an unknown number of times during the analytical session. We refer to the position of

changes in slope as "nodes" and define them as a function of mass bias and time. An advantage of this simple parameterization is that it can approximate a large range of complex functions by varying the positions and the number of the nodes. Although the parameterization is comprised of line segments, through high-density sampling of parameter space (as described below) the resulting calibration and it's uncertainty will be smooth functions, the final shape of which will be controlled by the structure of the input data.

In order to infer the probability of the locations of these nodes and an overdispersion term we adopt a transdimensional Bayesian framework[10,11]. In this framework, the posterior probability distribution of the model parameters is the distribution of interest, as it describes the positions of the nodes (and hence the distribution of the calibration through time) and the magnitude of the overdispersion parameter. The posterior probability distribution given the data is a product of the model likelihood function (which quantifies how well the data fit the model) and the prior distribution of the model parameters. For the likelihood function, we assume that each RM analysis is drawn from a normal distribution centered on the true, but unknown, value of the RM, with a variance of $\sigma^2 + \xi^2$, where σ^2 is the measured variance and ξ is the overdispersion[12]. In turn, the log-likelihood of a model is a function of the observed ratios (r_i), the predicted ratios (p_i) and the overdispersion ξ:

$$L = -0.5 \sum_{i=1}^{n} \left[\frac{(r_i - p_i)^2}{\sigma_i^2 - \xi^2} + ln\left(\sigma_i^2 - \xi^2\right) + ln(2\pi) \right]$$

where n is the number of measurements of the RM.

The prior distribution quantifies what is known about the parameters "prior" to the analysis. Here, we assume that all parameters are independent and use what is referred to as a "weak" prior distribution, one that constrains the minimum and maximum values of the calibration to reasonable values but does not strongly control its final form. We assign a uniform density prior distribution to the "time" parameter between the maximum and minimum times defined by the analytical session. For the calibration itself, we also assign a uniform distribution that has maximum and minimum values that extend a reasonable distance above the highest and lowest measurements. Similarly, the prior distribution of ξ is uniform and must be defined between ξ_{min} and ξ_{max} (which we define based on the observed data spread).

In order to sample and approximate the posterior distributions of the calibration and ξ, we use a rj-MCMC algorithm[13]. Here, we provide a short description of the algorithm and the philosophy behind this approach, but refer readers to Sambridge et al.[9] for a more complete description. The rj-MCMC algorithm is similar to the MCMC algorithm, in which parameter space is explored in a sequential manner by proposing perturbations to a current model. The value of a perturbation is drawn from a proposal distribution, commonly described as a Gaussian distribution centered on zero, and the variance controls the proposed distance from the current model. For example, the value of a specific node describing the current calibration model may be perturbed to form a proposed calibration model. The proposed model is then accepted or rejected such that perturbations that lead to more likely models are always accepted while less likely models are accepted in proportion to the ratio of the current-proposed likelihood. Once a proposed model is accepted, this model replaces the current model and is saved and used to approximate

the posterior distribution. This process is typically repeated 1000s of times. Importantly, the variance of the proposal distribution controls the rate at which the algorithm samples parameter space not the final posterior distribution, provided sufficient models are proposed and accepted.

In the case of the rj-MCMC algorithm, additional proposals account for the possibility of adding (Birth proposal) or subtracting (Death proposal) a node[9]. Increasing the complexity of the model by adding an additional node likely leads to increased data likelihood and *vice versa*. Therefore, it may be expected that the rj-MCMC will lead to overly complex models. However the acceptance criteria accounts for this change in dimensionality and not just the change in likelihood. The simplified acceptance criteria is

$$\alpha = min\left(1, \frac{P(m_p)}{P(m_c)} \cdot \frac{L_p}{L_c}\right)$$

where m is a vector containing the model parameters (positions and values of nodes and the overdispersion) and $P(m)$ is the prior distribution of the model parameters, and L is the likelihood (or data misfit) and the subscripts p and c correspond to the proposed and current models. Although the ratio of the likelihoods, L_p/L_c, will tend to lead to more complex models, the prior ratio, $P(m_p)/P(m_c)$, will favor simpler models. For example, if a new node is proposed but the likelihood remains unchanged, L_p and L_c cancel, leaving only $P(m_p)$, which is equivalent to $P(m_c)$ multiplied by the prior on the new parameter, which is less than one. Therefore, the probability of this proposal being accepted is equal to the prior on the new parameter. This highlights that simpler models will be favored over more complex models with similar misfits. Note that this is a simplified explanation for illustrative purposes. The exact value of $P(m)$ is a complicated function of the width of the prior for permitted calibration values, the number of nodes describing the calibration and the width of the prior for overdispersion. For an in depth description of the rj-MCMC algorithm the reader is referred to[9] and for a description of how $P(m)$ is calculated the reader is referred to [14].

There are five distinct proposals that are possible: 1) the time value of a node can move (Move); 2) the value of the calibration at a node can change (Change); 3) the number of nodes describing the calibration can be increased (Birth); 4) the number of nodes describing the calibration can be decreased (Death); 5) the value of ξ defining overdispersion can change (Noise). Proposals (1-5) are highlighted in figure 3. The proposed perturbations are drawn from Gaussian distributions centered on the current model with specified standard deviations and these must be tuned to provide acceptance rates as close to 44% for each type of perturbation[15]. The initial models in the Markov chain form the "burn in" period prior to the chain achieving convergence, and this part of the chain is very sensitive to the first model, which is selected at random. Therefore, only these models are not used approximate the posterior distribution.

The multi-dimensional parameter space is projected onto a plane representing time and calibration drift. This is achieved by discretizing this plane into number of pixels with constant area. The number of times a model in the ensemble of accepted models intersects a specific pixel divided by the total number of these models provides the posterior probability that the calibration drift was that specific value at that specific time. Furthermore, we can characterize features of the distribution such as a mean value and Bayesian equivalents of confidence intervals. The mean value is approximated as the expected model, which is the weighted sum of the posterior distribution, we refer to this model as the mean below. The Bayesian equivalent of a confidence interval is a credible interval, which accounts for the prior

distribution. The 68 % and 95 % credible intervals are shown about the expected intervals. The overdispersion distribution can be visualized with a histogram of accepted models.

Example Results

To demonstrate the utility and validity of this technique, we provide four examples. The first two examples apply the technique to simple synthetic datasets to demonstrate that despite the apparent complexity of the rjMCMC technique, it accurately returns the true model parameters. The final two examples are real datasets for which the scatter in the calibration is a smooth but non-linear function of time.

Synthetic Data

In example A, there is no drift in the calibration and the prescribed measurement uncertainties capture all of the scatter in the calibration. For this example, 20 random values representing measurements were drawn from a Gaussian distribution with a mean of 1 and a standard deviation of 0.001. The "uncertainties" of the measurements were drawn from a lognormal distribution with a mean of 0.001 to simulate the real variation that is seen in measurement uncertainties. Example B is the same as example A, except that an additional component of constant magnitude overdispersion (ξ) of 0.002 has been added to the Gaussian distribution prior to sampling.

Example A

For example A, the rj-MCMC analysis recovers a calibration consistent with the assigned values. The calculated mean value is approximately equal to 1 and does not systematically deviate from this value as a function of time. The 68 % credible interval of the calibration, approximately equivalent to one standard deviation varies somewhat, but is close to +/-0.001, similar to the assigned value. The distribution of the predicted overdispersion has a broad maximum that extends from 0 to about 0.0005. Since this value would be quadratically added to single analysis uncertainties (which have a mean of 0.001) their effect is negligible, and practically equivalent to an overdispersion of 0, which is the assigned value.

Example B

In example B, again we predict the true values for the mean. In this case, while the 68 % credible interval is somewhat variable but is between ±0.001 and ±0.002, the latter being the assigned total scatter of the data. In contrast to example A, the overdispersion parameter is clearly separated from a value of zero, and the true value of overdispersion, 0.002 is captured by the distribution of ξ.

Pb isotope data

We now apply our approach, to the Pb isotope measurements discussed above (Figure 4a,b). The mean value of the calibration model captures the overall structure of the data. The distribution of the calibration has a relatively constant width at 68%, but has variable asymmetry and width at 95%, particularly at times when the calibration appears to be shifting. The distribution of the overdispersion strongly resembles that from Example A, which has a broad maximum extending from a value of zero before monotonically decreasing near the value of the typical analysis precision. This is a distribution that implies no or very little excess scatter. Therefore the analytical uncertainties account for the scatter in the data.

K Isotope data

For a final example, we show MC-ICPMS data of K isotope ratio measurements over the course of a 14 hour analytical session (Figure 4c,d). This dataset shows a number of interesting features, including a long period of nearly unchanging instrument calibration, a slow rise, and two substantial changes in slope. The rj-MCMC algorithm appears to capture the overall topology of the dataset quite well. The flat, unchanging portion is characterized by a precisely defined calibration, but at the strong inflection points the distribution becomes very broad and asymmetric. The consistency of the distribution is shown in the inset to Fig. 4c. In contrast to the Pb isotope data, the K isotope data show a substantial amount of overdispersion, approximately equal to the value of the typical analysis precision (Fig. 4d). This suggests that the reported variance of a measurement (if treated in an identical manner as the RMs) needs to be doubled or equivalently the uncertainty needs to be expanded by a factor of approximately 1.4.

Discussion

The results from the synthetic datasets demonstrate that despite the complexity of the rj-MCMC technique and the fact that it can allow for very complex models, the technique accurately recovers the true values and simple parameter distributions from straightforward datasets. In particular, the model performs well in resolving the tension between the attribution of overdispersion and model complexity and correctly attributes the extra scatter in the second synthetic example to overdispersion rather than complex instrument drift. This is important, because it shows that our technique is robust and can be applied to simple datasets (where traditional techniques also work well) as well as more complex cases where this technique excels.

We expect that datasets that have a low complexity but are highly overdispersed will challenge the rj-MCMC technique. However, datasets of this type (highly overdispersed) probably indicate a problem with either the measurements or the method by which the uncertainty is assigned, and should probably be addressed prior to treatment by any data reduction scheme.

The two real datasets are characterized by mean values that smoothly capture the overall trends in the data. The distributions of the calibration models are smooth, symmetric and close to Gaussian during periods in which the calibration is either unchanging or changing linearly, but near knickpoints the distribution widens and can become asymmetric, particularly in the tails. This feature of the distributions is a consequence of the lower confidence that the drift of the calibration is accurately captured by the model in these regions. Features such as non-linear changes and asymmetry in precision may be unfamiliar to some analysts, but they are a consequence of non-linear changes in mass bias.

A disadvantage of our approach is that it is relatively computationally expensive, as many thousands of models are required to approximate the posterior distribution. However, the computations involved in these calculations can be made in a couple of minutes on desktop personal computer.

Conclusions

We have developed a method to infer the probability of calibration drift through time along with an estimate of the overdispersion of the measured RM. Our approach uses a reversible jump Markov chain

Monte Carlo algorithm, which provides a means to simultaneously sample the calibration-time space, the model complexity and a term describing model overdispersion. The code used for the calculations is written in Fortran. These computations are straightforward enough to be run on inexpensive personal computers, and therefore can be built into general data reduction schemes, providing tools to analysts to make more accurate measurements.

Acknowledgements

We thank two anonymous reviewers for helpful comments. This work was supported by the Ann and Gordon Getty Foundation, and the Swiss National Science Foundation (P2EZP2_148793). We thank Leah E. Morgan for allowing us to use her unpublished K isotope data. We thank Thomas Bodin for stimulating discussions and help with the code. We would like to thank Paul R. Renne, Greg Balco, Warren D. Sharp, Alan L. Deino, David Shuster, Roland Mundil for useful discussions.

Figure Captions

Figure 1. Ambiguity associated with model selection when interpolating between twenty-seven measurements of $^{208}Pb/^{206}Pb$ of the reference material NIST SRM-612 glass by laser-ablation MC-ICP-MS. The analytical session is ~7 hour in duration. (A) A general trend is observed in the data during the course of the analytical session. (B) Interpolating between each pair of measurements does not enable estimation of uncertainty of the RM. (C) Regressing linear segments through portions of the time series does permit the uncertainty to be estimated, however it is unclear how many segments to use and how to treat adjacent segments.

Figure 2. Five changes to the current model (solid black lines) may be proposed at each step of the rj-MCMC. (A) Proposals 1, 2 and 5 are shown: the location of the node may move (dotted line), the ratio value of a node may change (dashed line), or the overdispersion may change. (B) Proposals 3 and 4 are shown: a new node can be proposed (dashed line) or a node can be removed (dotted line).

Figure 3. Application of our method for synthetic two synthetic datasets, examples A and B. Posterior probability of calibration drift through time for a synthetic dataset (A) with a mean of 1 and standard deviation of 0.001. A(i). Measurement uncertainty has been assigned to each datum assuming a log-normal distribution with a mean of 0.001. In A(i), the solid black curve shows the expected calibration through time, and the dark grey and light grey envelopes represent the 68 % and 95 % credible intervals, respectively. The histogram of overdispersion values for accepted models approximates the posterior probability of overdispersion in the data, A(ii). The true assigned overdispersion value is 0 as highlighted in the figure. The same figures are shown for example B. Posterior probability for calibration drift through time, B(i), for synthetic dataset (B) and, B(ii), histogram of overdispersion values.

Figure 4. Application of our method for two real datasets. The black line is the central tendency of the posterior distribution, and the dark and light grey are 68% and 95% credible intervals, respectively. (A) Measured $^{208}Pb/^{206}Pb$ of NIST SRM-612 glass by laser-ablation ICP-MS through time and the corresponding posterior probability of calibration drift. (B) Posterior distribution of overdispersion in the data. (C) Measured $^{41}K/^{40}K$ of NIST SRM-985 by solution MC-ICPMS through time with the corresponding posterior probability of calibration drift, with an inset showing a close up view of the posterior distribution. (D) Posterior distribution of overdispersion in the data.

References

1 K. K. Murray, R. K. Boyd, M. N. Eberlin, G. J. Langley, L. Li and Y. Naito, *Pure Appl. Chem.*, 2013, **85**, 1515–1609.

2 I. S. Williams, in *Applications of microanalytical techniques to understanding mineralizing processes*, eds. M. A. McKibben, W. C. Shanks III and W. I. Ridley, Society of Economic Geologists, 1998, vol. 7, pp. 1–35.

3 N. T. Kita, T. Ushikubo, B. Fu and J. W. Valley, *Chem. Geol.*, 2009, **264**, 43–57.

4 A. R. Date and A. L. Gray, *Int. J. Mass Spectrom. Ion Phys.*, 1983, **48**, 357–360.

5 F. Albarède, P. Telouk, J. Blichert-Toft, M. Boyet, A. Agranier and B. Nelson, *Geochim. Cosmochim. Acta*, 2004, **68**, 2725–2744.

6 T. F. D. Mason, D. J. Weiss, M. Horstwood, R. R. Parrish, S. S. Russell, E. Mullane and B. J. Coles, *J. Anal. At. Spectrom.*, 2004, **19**, 218–226.

7 C. Paton, J. D. Woodhead, J. C. Hellstrom, J. M. Hergt, A. Greig and R. Maas, 2010, *Geochemistry, Geophysics, Geosystems*,**11**, 1-36

8 W. Compston and S.W.J. Clement, 2006, *Applied Surface Science,* **252**, 7089–7095

9 M. Sambridge, T. Bodin, K. Gallagher and H. Tkalčić, *Philos. Trans. R. Soc. Lond. Math. Phys. Eng. Sci.*, 2013, **371**, 20110547.

10 A. Tarantola, *Inverse Problem Theory and Methods for Model Parameter Estimation*, SIAM, 2005.

11 D. Sivia and J. Skilling, *Data Analysis: A Bayesian Tutorial*, Oxford University Press, Oxford; New York, 2 edition., 2006.

12 P. Vermeesch, *Chem. Geol.*, 2010, **271**, 108–111.

13 P. J. Green, *Biometrika*, 1995, **82**, 711–732.

14 T. Bodin, M. Sambridge, H. Tkal**čić**, P. Arroucau, K. Gallagher, and N. Rawlinson *J. Geophys. Res., 2012,**171,*** B02301

15 G. O. Roberts and J. S. Rosenthal, *Stat. Sci.*, 2001, **16**, 351–367.

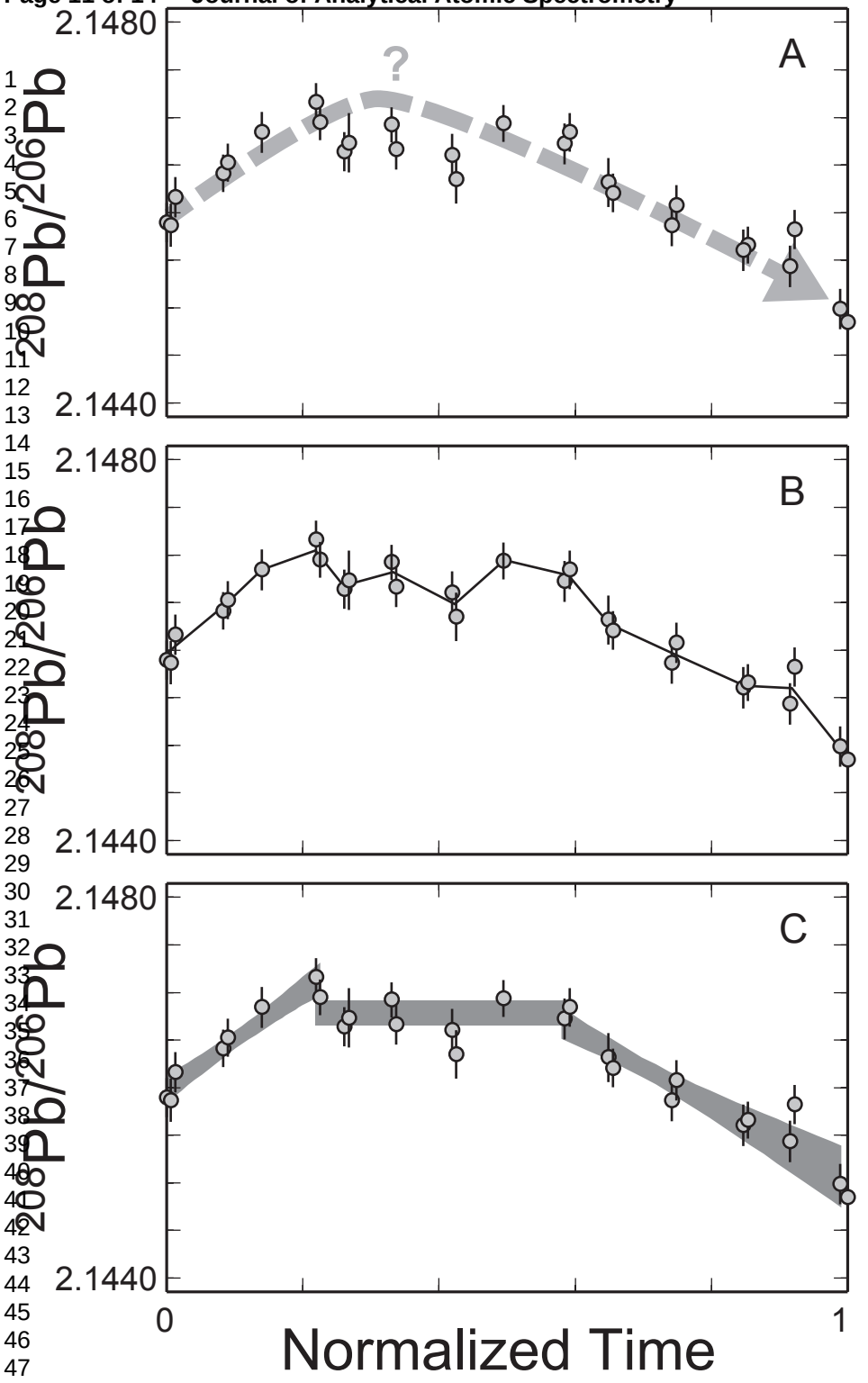
2.1480
2.1440
A
?
$^{208}Pb/^{206}Pb$
B
C
0
1
Normalized Time

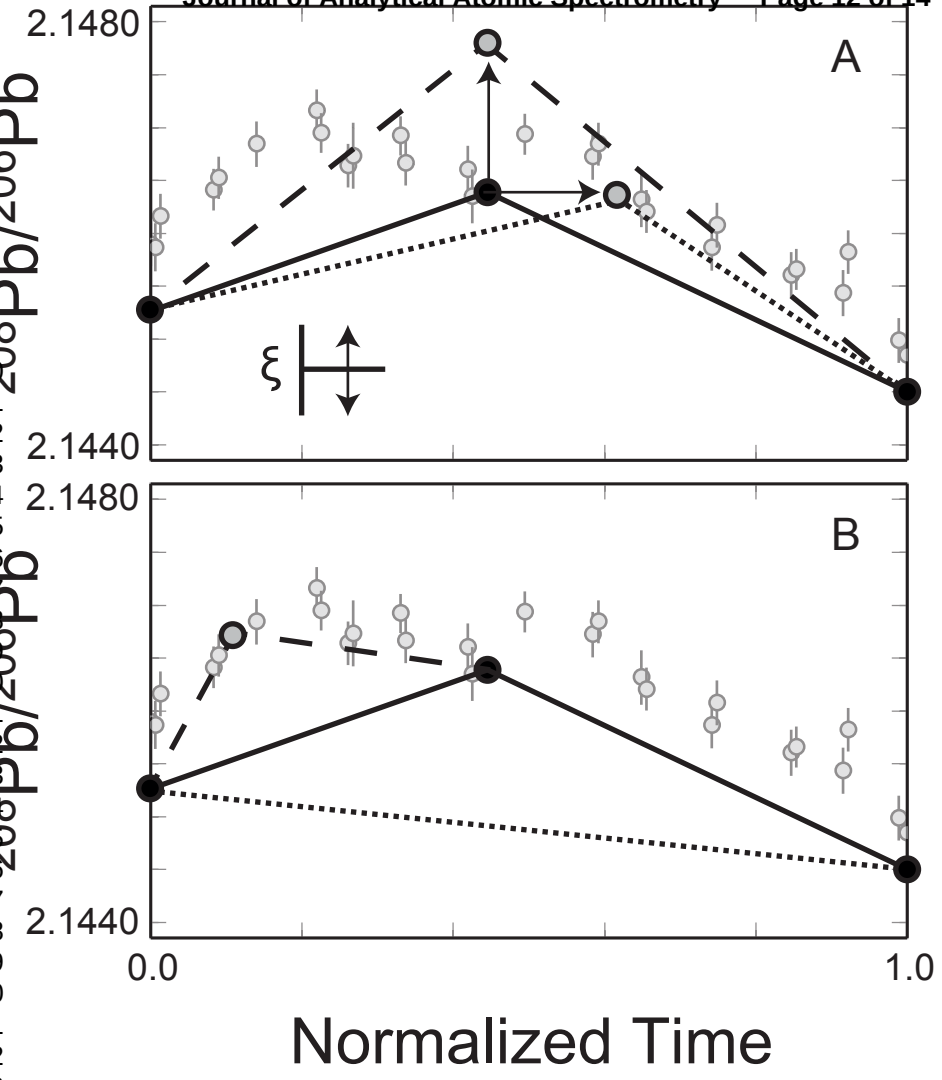
2.1480
A
$^{208}Pb/^{206}Pb$
2.1440
ξ
2.1480
B
$^{208}Pb/^{206}Pb$
2.1440
0.0
1.0
Normalized Time

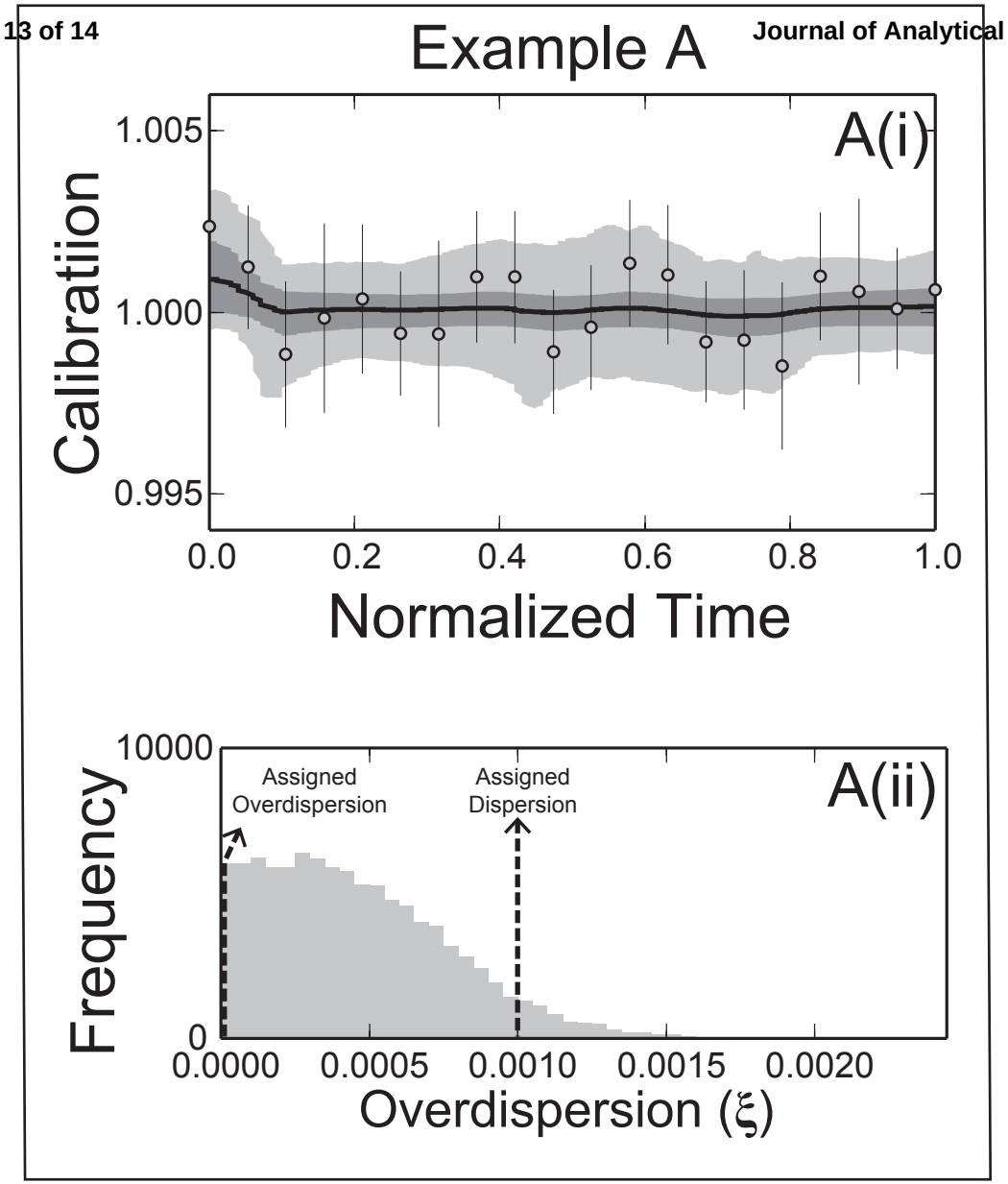
Example A
A(i)
Calibratiion
1.005
1.000
0.995
0.0
0.2
0.4
0.6
0.8
1.0
Normalized Time
A(ii)
Frequency
10000
0
Assigned Overdispersion
Assigned Dispersion
0.0000
0.0005
0.0010
0.0015
0.0020
Overdispersion (ξ)

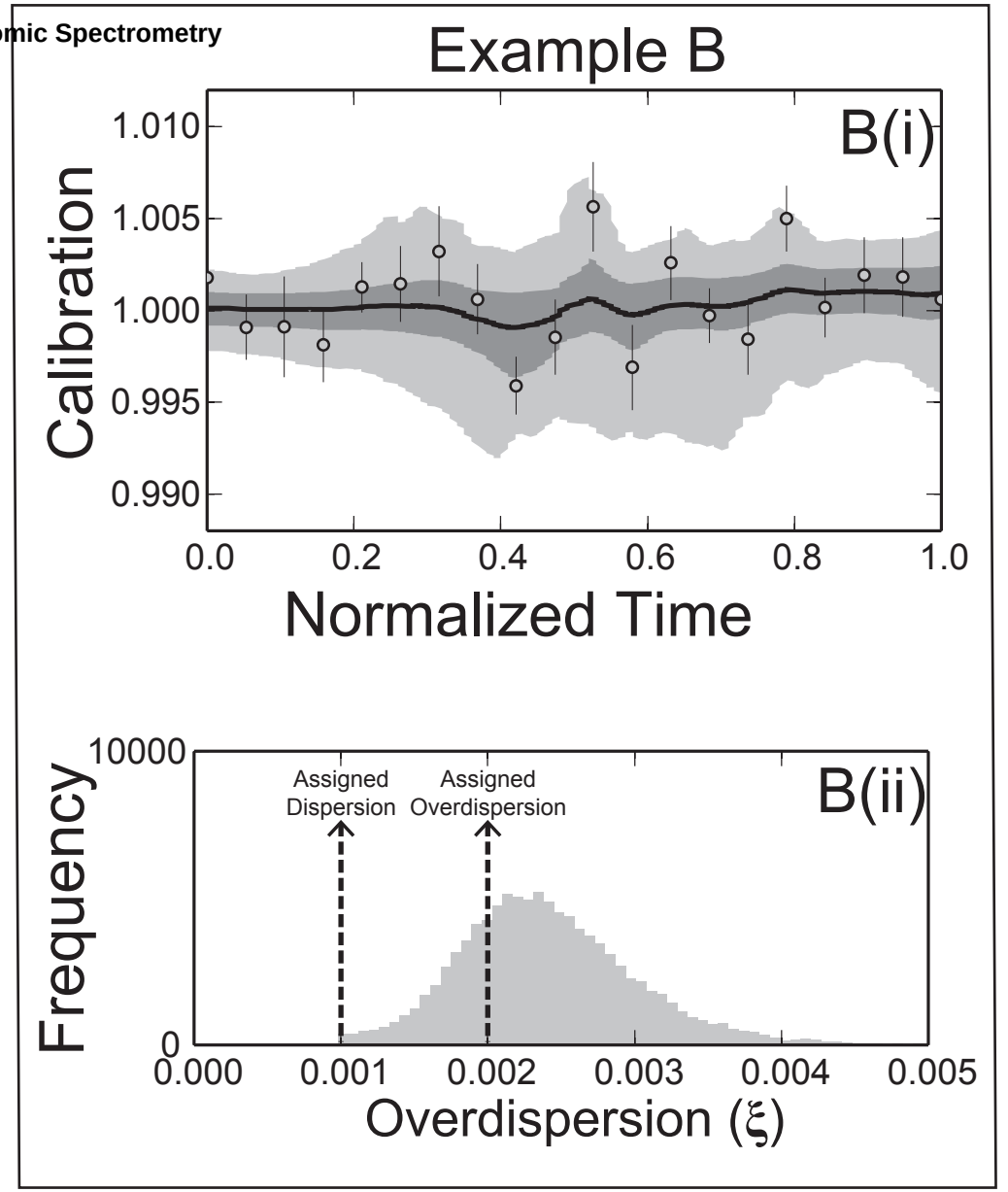
Example B
B(i)
Calibration
1.010
1.005
1.000
0.995
0.990
0.0
0.2
0.4
0.6
0.8
1.0
Normalized Time
B(ii)
Frequency
10000
0
Assigned Dispersion
Assigned Overdispersion
0.000
0.001
0.002
0.003
0.004
0.005
Overdispersion (ξ)

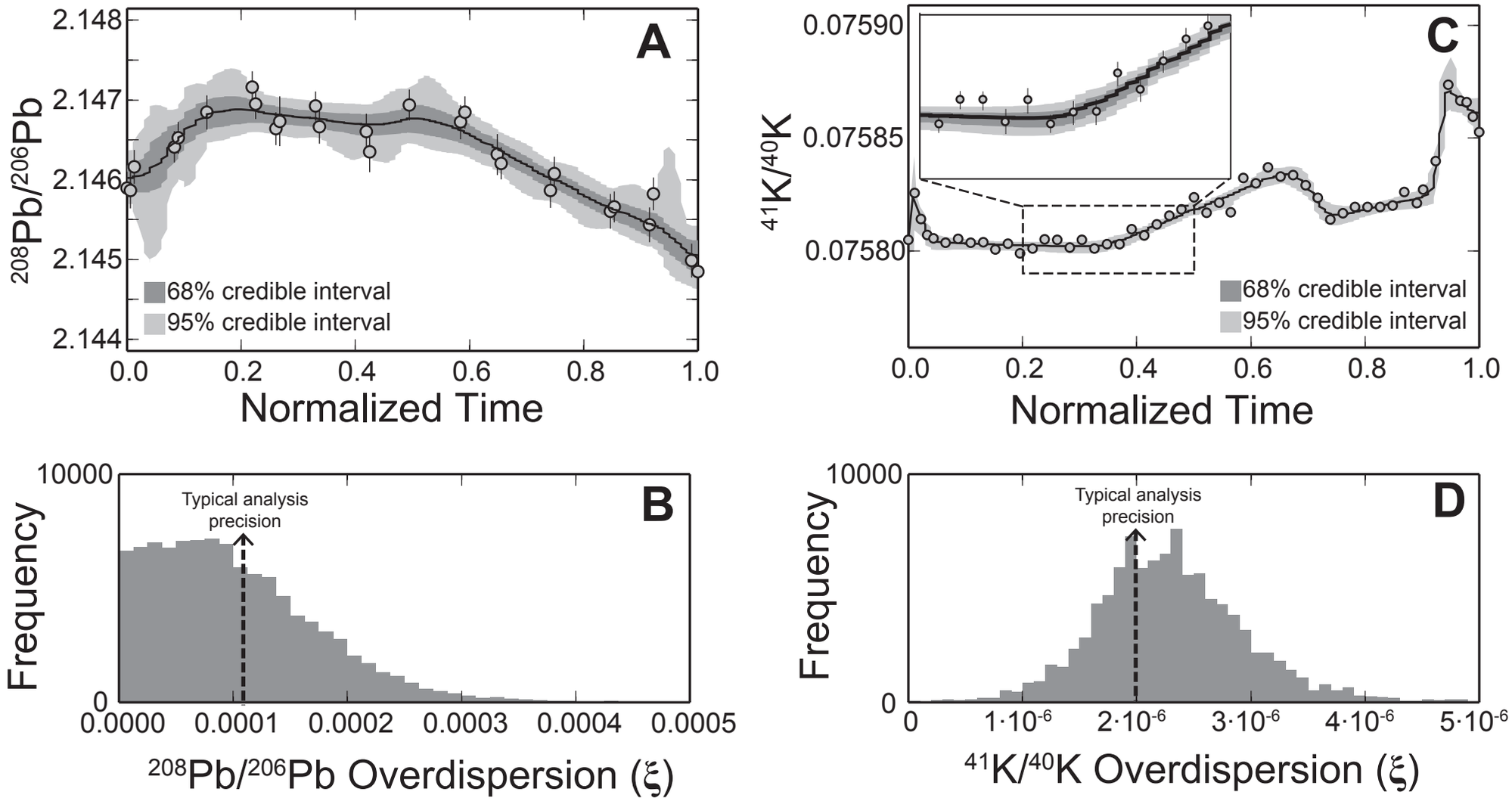
A
2.148
2.147
2.146
2.145
2.144
$^{208}Pb/^{206}Pb$
68% credible interval
95% credible interval
0.0
0.2
0.4
0.6
0.8
1.0
Normalized Time
C
0.07590
0.07585
0.07580
$^{41}K/^{40}K$
68% credible interval
95% credible interval
Normalized Time
B
10000
0
Frequency
Typical analysis precision
0.0000
0.0001
0.0002
0.0003
0.0004
0.0005
$^{208}Pb/^{206}Pb$ Overdispersion (ξ)
D
10000
0
Frequency
Typical analysis precision
$1\cdot10^{-6}$
$2\cdot10^{-6}$
$3\cdot10^{-6}$
$4\cdot10^{-6}$
$5\cdot10^{-6}$
$^{41}K/^{40}K$ Overdispersion (ξ)